SANDIA REPORT

SAND2011-2057
Unlimited Release
Printed January 2011

Laser Wafering for Silicon Solar

Thomas A. Friedmann, Bradley Jared, and Bill Sweatt

Prepared by
Sandia National Laboratories
Albuquerque, New Mexico 87185 and Livermore, California 94550

Sandia National Laboratories is a multi-program laboratory managed and operated by Sandia Corporation, a wholly owned subsidiary of Lockheed Martin Corporation, for the U.S. Department of Energy's National Nuclear Security Administration under contract DE-AC04-94AL85000.

Issued by Sandia National Laboratories, operated for the United States Department of Energy by Sandia Corporation.

Available to DOE and DOE contractors from
U.S. Department of Energy
Office of Scientific and Technical Information
P.O. Box 62
Oak Ridge, TN 37831

Telephone: (865) 576-8401
Facsimile: (865) 576-5728
E-Mail: reports@adonis.osti.gov
Online ordering: http://www.osti.gov/bridge

Available to the public from
U.S. Department of Commerce
National Technical Information Service
5285 Port Royal Rd.
Springfield, VA 22161

Telephone: (800) 553-6847
Facsimile: (703) 605-6900
E-Mail: orders@ntis.fedworld.gov
Online order: http://www.ntis.gov/help/ordermethods.asp?loc=7-4-0#online

SAND2011-2057
Unlimited Release
Printed March 2011

Laser Wafering for Silicon Solar

Thomas A. Friedmann (PI)
Nanomaterials Sciences Department

William C. Sweatt
Sensing and Imaging Technologies

Bradley H. Jared
Organic Materials Department

Sandia National Laboratories
P. O. Box 5800
Albuquerque, NM 87185-0352

Abstract

Current technology cuts solar Si wafers by a wire saw process, resulting in 50% "kerf" loss when machining silicon from a boule or brick into a wafer. We want to develop a kerf-free laser wafering technology that promises to eliminate such wasteful wire saw processes and achieve up to a ten-fold decrease in the g/W_p (grams/peak watt) polysilicon usage from the starting polysilicon material. Compared to today's technology, this will also reduce costs (~20%), embodied energy, and green-house gas GHG emissions (~50%). We will use short pulse laser illumination sharply focused by a solid immersion lens to produce subsurface damage in silicon such that wafers can be mechanically cleaved from a boule or brick. For this concept to succeed, we will need to develop optics, lasers, cleaving, and high throughput processing technologies capable of producing wafers with thicknesses < 50 μm with high throughput (< 10 sec./wafer). Wafer thickness scaling is the "Moore's Law" of silicon solar. Our concept will allow solar manufacturers to skip entire generations of scaling and achieve grid parity with commercial electricity rates. Yet, this idea is largely untested and a simple demonstration is needed to provide credibility for a larger scale research and development program.

The purpose of this project is to lay the groundwork to demonstrate the feasibility of laser wafering. First, to design and procure on optic train suitable for producing subsurface damage in silicon with the required damage and stress profile to promote lateral cleavage of silicon. Second, to use an existing laser to produce subsurface damage in silicon, and third, to characterize the damage using scanning electron microscopy and confocal Raman spectroscopy mapping.

Acknowledgments

This work was performed under the Laboratory-Directed Research and Development (LDRD) program at Sandia National Laboratories (project 147486). The authors would like to thank Martin de Boer for help with silicon fracture mechanics, Mike Sinclair for help with the optics conception and design, Joel McDonald for initial laser damage work, Thomas Beechem for the Raman mapping work, and Jonathan Rivera for the SEM measurements.

Contents

1. Introduction 8
1.1. Technical Approach 8
1.1.1. Background 8
1.1.2. How laser wafering will meet DOE goals and enhance PV manufacturing 9
1.1.3. Degree of innovation as compared to the current state of the art 9
1.1.4. Idealized laser wafering process 11
1.2. Document Overview 12
2. Optics 13
2.1. Optics Considerations 13
2.1.1. Solid Immersion Lens for Tight Focusing 13
2.1.2. Intensity distribution at the focal plane 14
2.2. Optics Design 14
2.3. Optics Fabrication 17
2.3.1. Wedge fabrication 17
2.3.2. Silicon Immersion Lenslets 17
3. Laser Damage and Characterization 18
3.1. Laser damage 18
3.2. SEM Characterization 18
3.3. Raman Mapping 20
4. Conclusion 21

Figures

Figure 1.2 Schematic of laser wafering concept. Note that the top surface is not damaged or roughened allowing the next wafer to be processed immediately upon cleaving the first. 10
Figure 2.2 Subsurface focusing at high NA through the use of a solid immersion lens. 12
Figure 2.3 The Point Spread Function 13
Figure 2.4 Schematic of the optics design showing the expanded beam passing through the stacked wedge assembly prefocused by a conventional planoconvex lens with the final focus through the silicon solid immersion lens. 14
Figure 2.5 Aperture with spokes creating one of the laterally displaced diffraction patterns. 14
Figure 2.6 Calculated beam intensity at the focus and 1 and 2 μm above the focus produced by the wedge shaped optic in Fig. 2.5 Note the different intensity scales at the right. The intensity above the central spot 2 μm above the focus is very low. 15
Figure 2.7 Cartoon of the four focus spot patterns created by the stacked wedges. The arrows represent the wedge direction. Each beamlet produces seven central spots for a total of 28 spots. 15
Figure 2.8 The left photo shows the 4-plate wedge assembly mounted in an optic holder. The right photo shows the optic setup with the focusing lens and silicon sample mounted on the computer programmable scanning stage. 17

Figure 2.9 Design of the silicon immersion lens. 17
Figure 2.10 The left image is a plot of the interferometrically measured contour of the etched silicon immersion optic. The right graph shows a line trace of the optic revealing the radius of curvature. 18
Figure 3.2 Cross section SEM of silicon sample after subsurface laser damage with different focus depths. The left image shows increased surface damage due to higher laser intensity at the silicon surface. 19
Figure 3.3 Histogram of the average damage depth and length of damage track as a function of focus depth. The focus position was adjusted to deeper depth from left to right. 19
Figure 3.4 Cross-sectional Raman mapping of nanosecond laser damage in silicon using a conventional focus lens assembly. The left image shows the Raman peak position map that is sensitive to the stress state in the material. The right image shows the FWHM that is a measure of the induced disorder. 20

Table

Table 1.1 Comparison of kerfless wafering technologies 10

Laser Wafering for Silicon Solar

1. INTRODUCTION

The purpose of this project is to explore the initial development of a kerf-free laser wafering technology that promises to eliminate wasteful wire saw processes and achieve up to a ten-fold decrease in the g/Wp polysilicon usage from the starting polysilicon material. Compared to today's technology, this will also reduce costs (~20%), embodied energy, and GHG emissions (~50%). We plan to use short pulse laser illumination sharply focused by a solid immersion lens to produce subsurface damage in silicon such that wafers can be mechanically cleaved from a boule or brick. For this concept to succeed, we need to develop optics, lasers, cleaving, and high throughput processing technologies capable of producing wafers with thicknesses < 50 μm with high throughput (< 10 sec/wafer). Wafer thickness scaling is the "Moore's Law" of silicon solar. Successful development of this concept will allow solar manufacturers to skip entire generations of scaling and achieve grid parity with commercial electricity rates.

1.1. Technical Approach

1.1.1. Background

The silicon photovoltaics industry has reduced the cost per watt peak ($/$W_p$) significantly from its birth in the early seventies with prices decreasing from near 100 $/$W_p$ then to values less than <1.50 $/$W_p$ today. This reduction in costs has followed an experience curve of ~0.8 over the years meaning that with every doubling of production volume comes a 20% reduction in cost. The largest deviation from this trend occurred recently (2006-2008) when the increasing volume of module production ran up against a shortage of polysilicon. For years the PV industry was small enough that it could rely on waste polysilicon from the larger semiconductor industry that could be obtained for ~$20/kg. Around 2005 this situation changed dramatically as polysilicon usage by the PV industry overtook that of the semiconductor industry leading to massive shortages and an increase in polysilicon prices near $100/kg and spot prices as high as $500/kg in 2008. Recently, the situation has eased with the current recession coupled with significantly greater polysilicon production prompting spot prices to collapse to <$60/kg.

Currently, both the PV and semiconductor industries rely on wire saws for slicing boules of silicon into wafers. A thin tension-controlled wire bathed in a slurry of SiC particles dispersed in a glycol solution is drawn across the boule such that the entire boule is cut in parallel with state of the art saws allowing for concurrent slicing of multiple boules. Thus, one saw can cut many (>5000) wafers per run with an average run rate of one wafer every 5-10 seconds. The current standard for wafer thickness is ~180 μm with a wire diameter of ~120 μm and wire length of 1100 km.[i] In addition, the cutting process typically creates microcracks that weaken the wafers requiring a damage wet etch of ~10-15 μm thickness (for both sides) to prevent yield loss from breakage. *Thus, the resulting kerf loss is nearly half of the total polysilicon boule.* Further scaling of wire saws to yet thinner wafers is possible, but there are practical limits on the wire thickness due to the tension required to produce uniform parallel cuts.

In addition, thin wafers are quite flexible, weak, and tend to stick to each other due to capillary action from the slurry, and thus singulation becomes a problem resulting in additional yield loss.

To summarize, wire saws are inherently wasteful of polysilicon, generate unwanted waste streams (slurry, acid wet etch), and due to microcracks are not scaleable to very thin wafers. What is needed is a kerfless technology that has a similar throughput and cost but can generate high strength wafers.

1.1.2. How laser wafering will meet DOE goals and enhance PV manufacturing

If successful, laser wafering will accelerate the adoption of PV in the US by reducing the material costs associated with polysilicon usage (2-10x), eliminating manufacturing costs associated with wire saws, and greatly reducing slurry and damage etch waste streams. This in turn will reduce module energy payback times to well below 1 year and also per watt greenhouse gas emissions associated with polysilicon production.

The commodity business of polysilicon production is well known for its boom and bust cycle. Reduced dependence on polysilicon consumption will smooth out the affects of this cycle on the PV industry leading to a more predictable growth pattern that should allow for better planning and increased consumer and investor confidence. More broadly, this technology should also be applicable to multicrystalline silicon and III-V materials such as Ge or GaAs where substrate costs are of even greater concern.

We also believe that laser wafering technology can be introduced in either an evolutionary and/or revolutionary manner because we will be able to generate wafer thicknesses spanning the range from 20-180 μm. Wafer manufacturers discovered that wire sawn wafers at the ~150 μm thickness were much harder to handle causing yield to suffer due to breakage, and with the decline in polysilicon spot prices in 2009 many manufacturers went back to 180 μm thickness wafers. This points to the need to develop industrial scale processes for thinner wafers such as wafer handling and innovative processing (e.g. light trapping, reducing wafer bow due to stress). No matter the process technology, we believe it will be possible to use the same laser wafering process ensuring that wafering issues will not limit PV development.

1.1.3. Degree of innovation as compared to the current state of the art

1.1.3.1. Kerfless String Ribbon Processes

The issues with wire saws are well known in the PV industry and have been discussed above. There are several competing kerfless processes that are in various stages of development. One subset is the well-known ribbon technologies[ii] (see Table 1). These are String Ribbon (SR), Edge-defined film growth (EFG), Crystallization on Dipped Substrate (CDS), Ribbon Growth on Substrate (RGS) and Ribbon on Sacrificial carbon Template (RST). All of these technologies produce multicrystalline wafers that suffer from impurity incorporation (mainly oxygen and carbon) with the average grain size tending to decrease with throughput; nevertheless, with effective hydrogen passivation efficiencies of these technologies are approaching or equal to multicrystalline cast silicon wafers, with potentially high (>90%) polysilicon utilization. In production, none of these technologies are making thin (<150 μm) wafers.

1.1.3.2. Weak Layer Kerfless Processes

A second class of kerfless technologies is based upon creation of a buried weak layer used to remove the silicon overlayer through mechanical cleaving or chemical etching[iii] (see

Table 1). In general, these methods allow for the use of high quality single crystal Si and potential efficiencies should equal or improve on the current cz-silicon thick silicon technologies. Sigen is using hydrogen ion implantation to create weak layers in crystalline silicon. The wafer is then mechanically cleaved form the brick. This process can produce large area wafers with smooth surfaces, but requires vacuum batch processing and it is unclear if it will be feasible on a commercial level particularly in regards to throughput. In addition, the ion implantation voltage increases with thickness, and rather high voltages (> 5 MeV) are required to produce wafers of thickness greater than 100 μm suggesting that this technology is best suited to very thin wafers. Similarly less developed methods such as epitaxially grown Si on a weakened porous Si layer also require vacuum batch processing through deposition of rather thick (~20 μm) PECVD Si layer. The recently introduced stress-induced lift off method (SLIM-Cut) does not require vacuum processing, but is relatively new and no data exists as to the efficiency of the method. We suspect that controlling the wafer thickness and roughness will be difficult, and the process requires a high temperature anneal and generates liquid waste.

Table 1.1 Comparison of kerfless wafering technologies

Kerfless Ribbon[ii]	**Acronym**	**Company**	**Wafer Thick.(μm)**	**In production**	**Microstructure**	**Throughput**
String Ribbon	SR	Evergreen Solar	150	Y	Multcrystalline	Low
Edge-defined Film Growth	EFG	Wacker-Schott	150	Y	Multicrystalline	Low
Crystallization on Dipped Substrate	CDS	Sharp	150	N	Multicrystalline	High
Ribbon Growth on substrate	RGS	ECN	150	N	Multicrystalline	High
Ribbon on sacrificial template	RST	Solarforce	80-150	N	Multicrystalline	Med.
Weak-Layer Methods[iii]						
Epi-growth on porous Si		ZAE Bayern	10-20	N	Single	Low
Smart Cut	Polymax	SIGEN	20-150	N	Single	Low
Stress-Induced Lift Off	SLIM-Cut	IMEC	20-100?	N	Single	Low?
Laser Wafering	LW	SNL	20-150	N	Single	Med/High?

1.1.3.3. Advantages of Laser Wafering

Our proposed laser wafering technology offers a vacuum-free process with the possibility of scaling easily with wafer thickness from the present standard down to the thinnest wafers. Liquid waste streams will be minimized and any scrap material generated will be easily recyclable. Also, by tailoring the laser parameters we may be able to produce wafers with controlled roughness for enhanced light trapping; and, by guiding the crack through the wafer, we will control out-of-plane deviations that will lead to increased wafer strength.

1.1.4. Idealized laser wafering process

We intend to produce silicon wafers by focusing a short pulse laser into a polished silicon brick (Figure 1.2) creating a planar damaged region weak enough to allow the entire wafer to be controllably cleaved from the brick. Once a wafer has been cleaved, the process can be repeated till the entire brick is used up. By controlling the laser parameters (pulse length, intensity, focused spot shape, etc.) we will be able to tailor the damage spots such that in-plane cracks of sufficient length are developed and that the resulting wafers have high strength.

There are many unknowns that must be addressed to assess the utility of the laser wafering concept. The purpose of this project was to produce damage in silicon using short pulse lasers in a controlled manner demonstrating the feasibility of the laser wafering approach. The essential concept, the creation by short-pulse laser of a buried highly-uniform weakened layer in a large area silicon brick or boule, to our knowledge has not been attempted. We believe that short pulse lasers hold the key to producing this damaged layer and have structured our proposal to address this issue. The laser beam delivery optics must be engineered to produce a tightly focused spot in such a manner that lateral cracks are generated. A wide parameter space of possible laser and focus conditions must be explored to optimize the crack generation process. Also, cleaving the wafer along the weakened layer must be demonstrated and optimized. This raises questions related to crack interactions along the cleave, and the ultimate surface roughness possible with such a scheme. Finally, thin wafers must be strong enough to handle for subsequent processing, which will only be possible if we are able to limit vertical crack development.

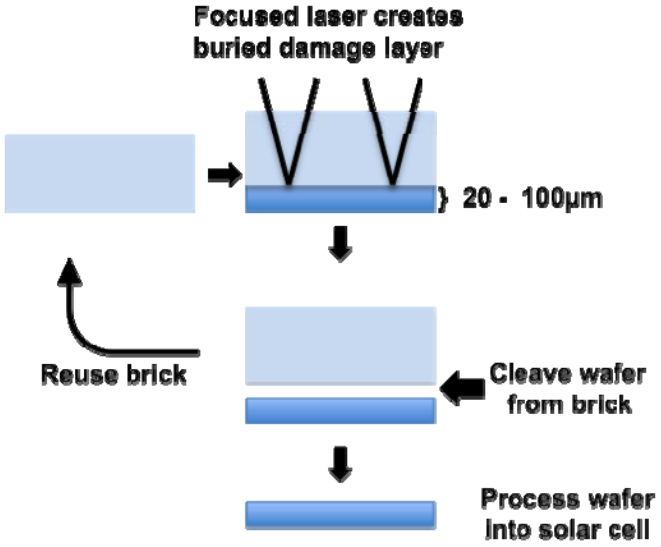

Figure 1.1 Schematic of laser wafering concept. Note that the top surface is not damaged or roughened allowing the next wafer to be processed immediately upon cleaving the first.

Nonlinear absorption effects are associated with the high peak powers of femtosecond laser pulses. Nonlinear optical interactions such as multi-photon absorption and Zener tunneling[iv] can seed avalanche ionization, providing the ability for femtosecond laser pulses to damage at laser wavelengths where corresponding photon energies are less than the bandgap of the material. For example, Si has a bandgap of 1.1 eV. At sufficient intensities, multiphoton absorption of 2 photons at a wavelength 2100 nm, or energy 0.59 eV, can be absorbed by an electron in the valence band of Si and promote it to the conduction band, thereby facilitating avalanche ionization and permanent material damage[v]. Furthermore, since these non-linear absorption processes are intensity dependent, they can be confined to a very limited volume at

the focus of an optic within the bulk of a material, producing damage regions far smaller than the diffraction limit.[iv]

1.2. Document Overview

The project work that follows starts with a broader discussion of the optical issues involved in laser wafering followed by the more practical design issues that guided our fabrication decisions, and a description of the fabricated optics. This is followed by a discussion of the subsurface laser damage and characterization.

2. OPTICS

2.1. Optics Considerations

A variety of optical components must be developed to enhance and optimize the kerfless laser wafering technique. The following sections provide an introduction to immersion lenses for precise focusing of infrared laser beams within silicon, and diffractive optics techniques to provide for a high throughput, parallel approach.

2.1.1. Solid Immersion Lens for Tight Focusing

The laser must be focused to the smallest possible spot size to minimize the thickness of the damage layer. This can be achieved through the utilization of a "solid immersion lens" (Fig. 2-2). The immersion lens itself must be roughly hemispherical, and be in optical contact with the surface of the silicon boule. It is the final optic in a fast, multi-element, multi-group lens that should be designed specifically for the purpose of bringing near IR light to an extremely sharp focus below the surface of a silicon boule. Note that to allow for penetration depths of several millimeters, we are restricted to wavelengths longer than the (indirect) bandgap of silicon $\lambda_{cutoff\text{-}Si}$ ~1.1μm.

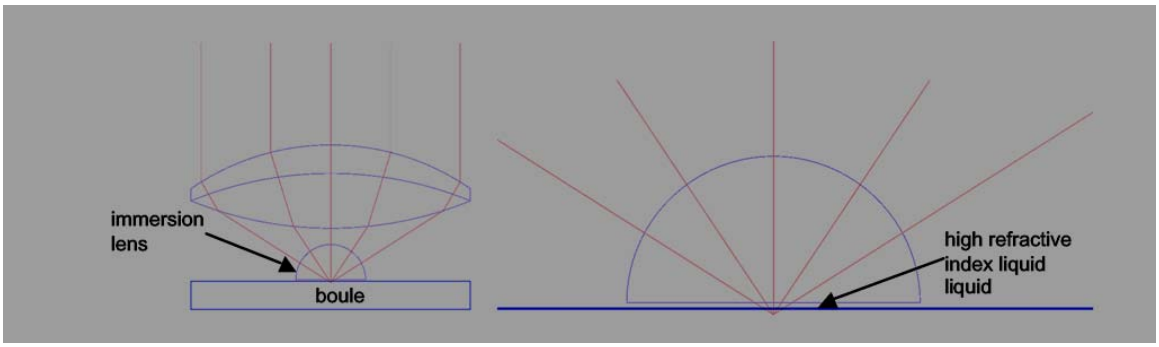

Figure 2.1 Subsurface focusing at high NA through the use of a solid immersion lens.

The use of immersion lenses along with immersion oil is commonplace in optical microscopy. The refractive index of the immersion oil enables a higher numerical aperture and thus increases resolution. The spot diameter (d_{Airy}) is related to the numerical aperture ($NA=n_{im}\sin\Theta$) through:

$$d_{Airy} = \frac{2.44\lambda}{NA} \qquad (1)$$

Where λ is the laser wavelength, n_{im} is the refractive index of the immersion medium, and Θ is the half angle of the converging laser beam. The refractive index of the immersion oil used in conventional microscopy is approximately 1.5. By utilizing a solid immersion lens of silicon with a refractive index of approximately 3.7, the spot size can be potentially reduced by ~2

times. Using a silicon immersion lens would, in principle, allow us to achieve a lateral spot diameter of approximately ~0.7 μm using ~1 μm laser radiation, with the axial extent of the focused spot approximately 1.5 times larger. In practice, we will likely utilize the lens at a somewhat lower numerical aperture to allow us to project multiple laser foci within the boule and to allow us to utilize beam shaping phase masks (see below). Finally, to enable the production of damaged zones at variable distances below the surface of the boule, an adjustable system for compensating variable amounts of spherical aberration must be developed.

2.1.2. Intensity distribution at the focal plane

The intensity distribution associated with a diffraction-limited focused beam is far from ideal for our purposes. Eighty-four percent of the pulse energy is deposited in the Airy disk with 7% in the first diffraction ring, etc. Furthermore, the intensity builds up as one approaches the ideal focal plane so material breakdown may start at the best focus but then it will propagate up the beam producing quite a cucumber-shaped damage pattern aligned with the beam centerline.

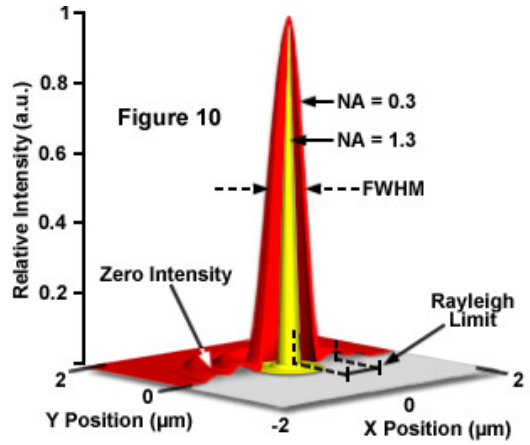

Figure 2.2 The Point Spread Function

What is desired is a pancake-shaped intensity profile whose surface is perpendicular to the beam centerline. This implies that we want to concentrate most of the flux in the (1st, 2nd, & 3rd?) diffraction rings with very little laser fluence crossing (and focusing on) the centerline.

One starting point for this design would be a diffraction-limited beam and a diffraction-limited lens. We would aberrate the laser beam before it enters the lens with a fused-silica plate with (we think) a half-wave step patterned on it. We think that the step should be radially symmetric starting at r/r_0=70%. We may also want to add a small symmetric obscuration on-axis.

We will model the intensity pattern with the lens design code ZEMAX. ZEMAX can easily model symmetric phase profiles and then we can step through focus looking for hot zones. Hopefully we will not need non-symmetric phase profiles but they are still reasonable to model. Somewhere in this design space we will find a system that creates a relatively "flat" intensity pattern.

The phase plates for this experiment can certainly be made by masking a fused silica plate and then depositing a step of SiO2 on the exposed surface. This approach will yield smooth surfaces on both the substrate and the step.

2.2. Optics Design

For this project a simpler method of spreading the focused beam into a more pancake shape was developed. Fig. 2.4 is a schematic of the optical design. The expanded 12 mm

diameter beam is passed through a 4-optic stacked wedge assembly that produces four slightly off-axis beamlets. These beamlets are then focused through a 50 mm lens onto the smaller silicon solid immersion lens that is designed to lay on the silicon wafer surface.

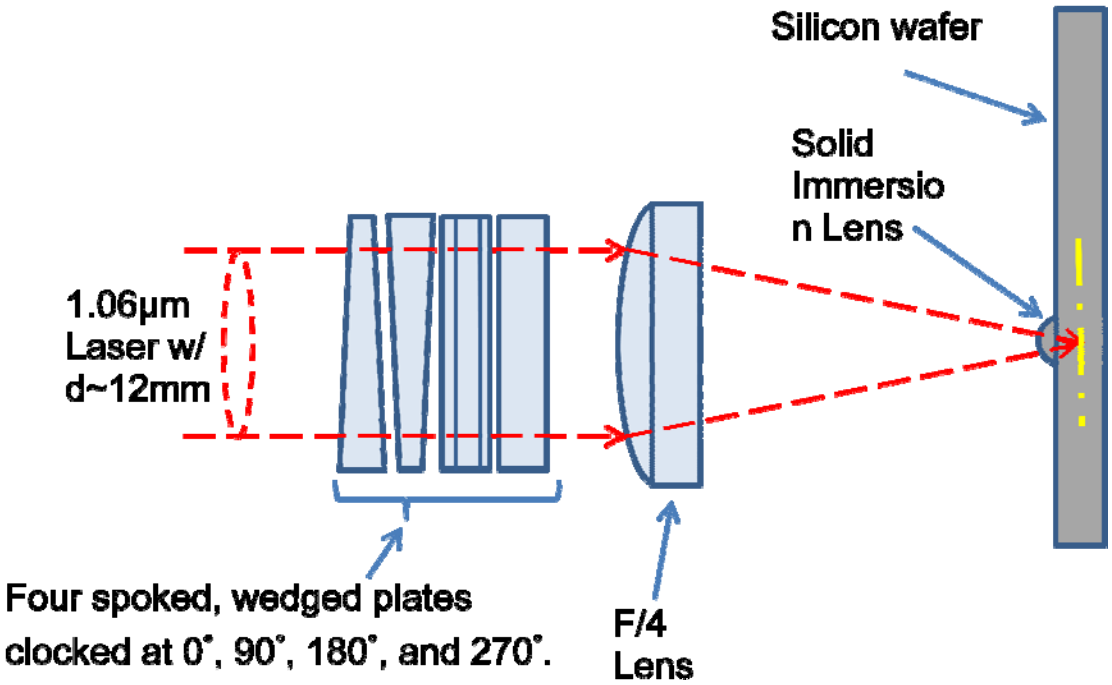

Figure 2.3 Schematic of the optics design showing the expanded beam passing through the stacked wedge assembly prefocused by a conventional planoconvex lens with the final focus through the silicon solid immersion lens.

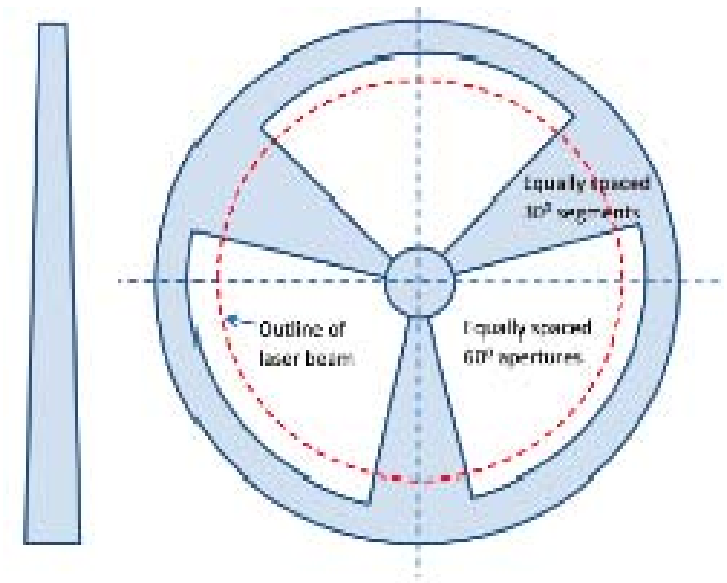

Figure 2.4 Aperture with spokes creating one of the laterally displaced diffraction patterns.

Fig. 2.5 shows a side and planview of one of the wedge shaped optics with three pie-shaped clear areas machined from the planar surface. The expanded laser beam passing through this optic will be deflected off-axis. The parts of the beam passing through the clear pie shaped areas will be undeflected, thus only a portion of the beam is split off from the main beam by this optic to be focused by the subsequent conventional lens and finally by the solid immersion lens.

A calculation of the focus pattern is shown in Fig. 2.6 at three different positions. The focused

pattern consists of 7 major spots with a central maximum spot surrounded by six less intense spots. At 2 μm above the focus the greatest intensity is less than 20% of the maximum intensity at focus. Importantly, the light intensity above the most intense central spot at focus is very low. This should help localize the thermal breakdown event to the focal plane, helping to limit undesirable out-of-plane melting.

Finally, By stacking four of these plates with 90° rotation one then produces four off-center beams that can be focused in-plane (Fig. 2.7), thus spreading the beam intensity profile. This design deposits the laser flux into a ~50-100 μm^3 volume. This volume can be changed by increasing or decreasing the focal length of the lens. By spreading the beam intensity at focus the objective is to flatten the profile of the melted silicon region and thus produce more planar damage that should be more effective in producing clean lateral cleavage of silicon.

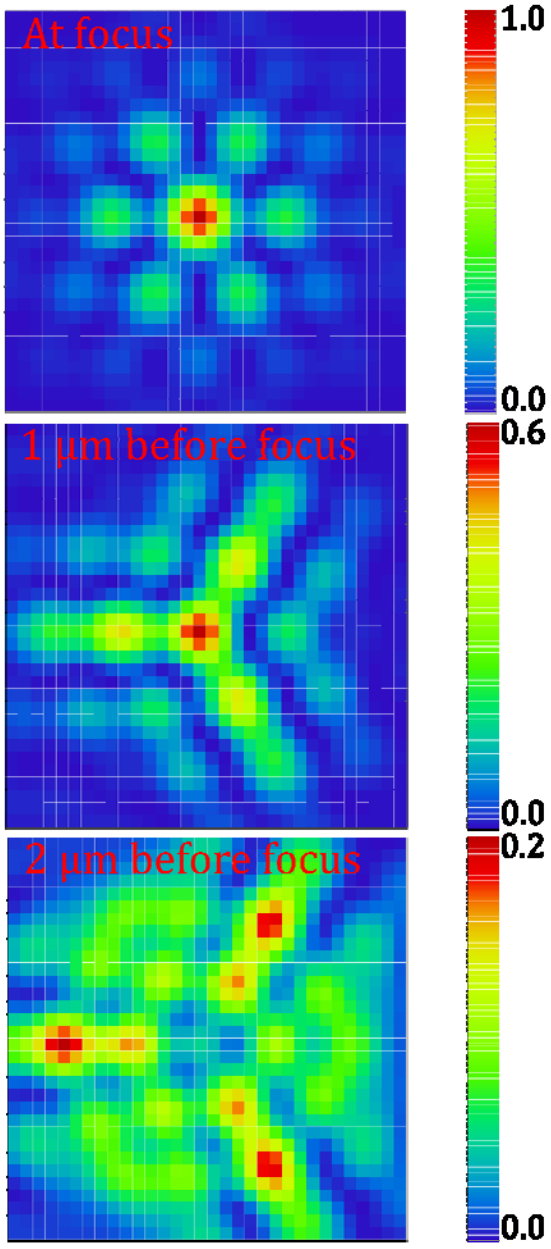

Figure 2.5 Calculated beam intensity at the focus and 1 and 2 μm above the focus produced by the wedge shaped optic in Fig. 2.5 Note the different intensity scales at the right. The intensity above the central spot 2 μm above the focus is very low.

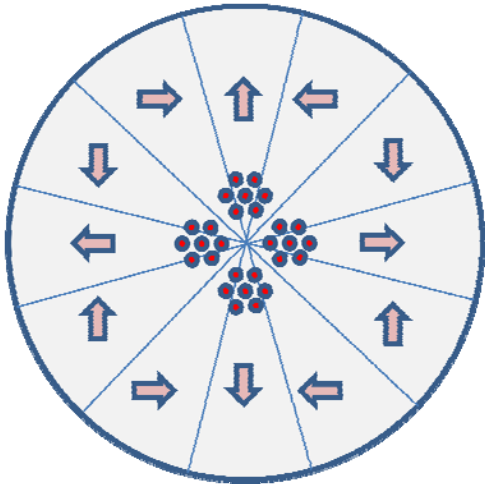

Figure 2.6 Cartoon of the four focus spot patterns created by the stacked wedges. The arrows represent the wedge direction. Each beamlet produces seven central spots for a total of 28 spots.

2.3. Optics Fabrication

2.3.1. Wedge fabrication

Fig. 2.8 is a picture of the fabricated wedges assembled into an optical holder. The

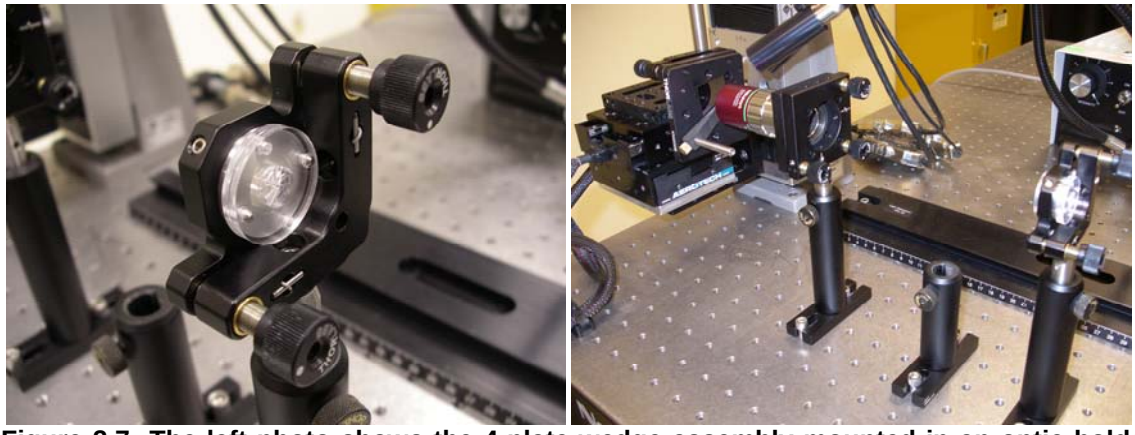

Figure 2.7 The left photo shows the 4-plate wedge assembly mounted in an optic holder. The right photo shows the optic setup with the focusing lens and silicon sample mounted on the computer programmable scanning stage.

wedge optics used to create the off-axis beamlets were fabricated using a diamond turning machine at Sandia. The wedges were made from IR transparent PMMA material. Four precision holes were drilled at the optic edges for the insertion of pins to ensure the proper rotational alignment. Fig. 2.8 also depicts a picture of the assembled optic train with the focusing conventional lens and the silicon sample mounted on a translational stage.

2.3.2. Silicon Immersion Lenslets

Fig. 2.9 is a schematic of one design of the silicon immersion lens appropriate for the conventional optic train discussed above. The optic is pictured fabricated on top of a conventional silicon semiconductor wafer. The dimensions of the optic are such that it is possible to consider techniques other than conventional machining for fabrication. One appealing concept is to manufacture arrays of lenslets on a thinned wafer that can then be placed on top of a silicon boule thus opening up the prospect of using multiple laser beams in parallel for producing damage spots.

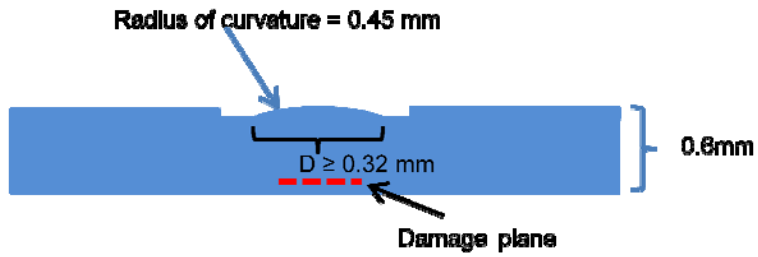

Figure 2.8 Design of the silicon immersion lens.

Fabrication of the silicon immersion lenses was also done at Sandia using a novel technique based on laser assisted plasma etching.

In this technique, chlorine gas is activated using a green laser focused on the silicon sample surface to produce locally high etch rates. The laser is then rastered across the sample surface in a programmed manner controlling the local etch depth by adjusting the dwell time of the laser. Complex shapes are typically built up layer by layer, and the surface roughness can be controlled by dithering the laser across individual steps. This technique is capable of removing 10^5 μm^3 of silicon per second allowing for the capability of fabricating lenslets and lenslet arrays directly in silicon material. Fig. 2.9 is an interferometrically measured height profile of a fabricated lenslet along with a surface profile scan showing the radius of curvature. The measured radius agrees quite well with the design radius. This technique can be used to make lenslets of different size and focal length ideal for prototyping purposes. The initial lenslets were fabricated such that the laser focus was within the underlying silicon. Thus, eliminating issues that might occur by imperfect matching of the silicon lenslet undersurface to the silicon wafer to be damaged.

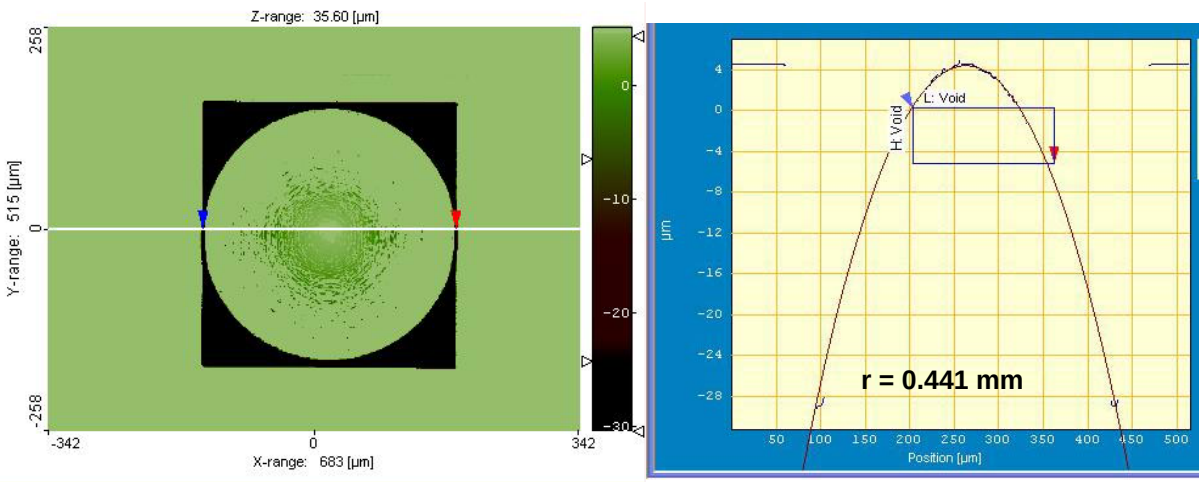

Figure 2.9 The left image is a plot of the interferometrically measured contour of the etched silicon immersion optic. The right graph shows a line trace of the optic revealing the radius of curvature.

3. LASER DAMAGE AND CHARACTERIZATION

3.1. Laser damage

A 10 ns laser was used to perform initial subsurface damage in Si(100) wafers. The laser was rastered across the silicon surface and the focus depth was adjusted to provide varying subsurface damage zones.

3.2. SEM Characterization

The Si sample was then cleaved and the damage imaged using a SEM microscope. In Fig. 3.2 the left image shows columnar damage in the sample consistent with a breakdown event occurring at depth followed by rapid heating up the core of the laser pulse similar to previous results. The right image in Fig 3.2 shows damage done with the laser focused more deeply into the. By comparing the two images one can see that the damage column on the left is longe than

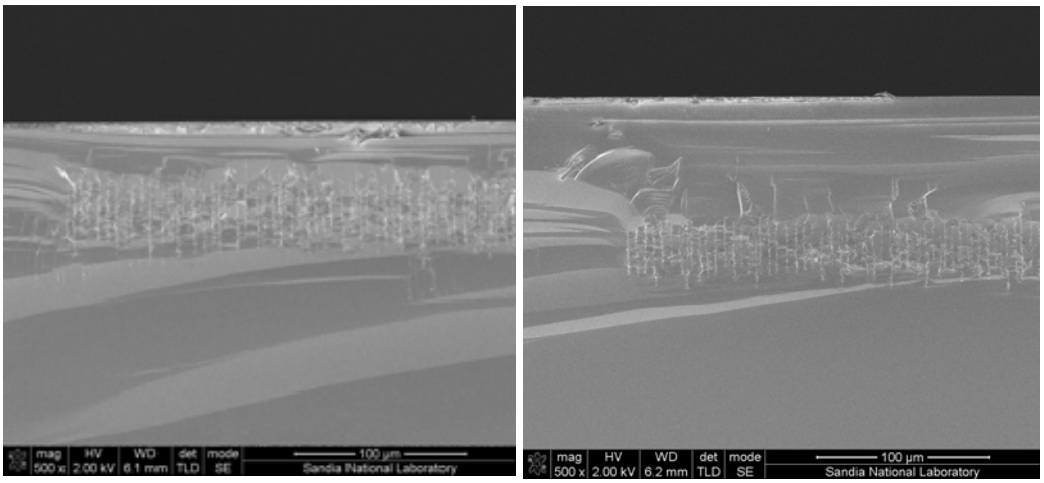

Figure 3.1 Cross section SEM of silicon sample after subsurface laser damage with different focus depths. The left image shows increased surface damage due to higher laser intensity at the silicon surface.

that on the right. This is readily explained by considering the absorption coefficient of silicon (10 cm^{-1}) at the laser wavelength of 1064 nm. At the deeper depth more light is absorbed prior to the focus, leaving less energy for producing the columnar damage zone. Correspondingly, at the shallower depth less light is absorbed before the focus leading to greater energy available to create a longer damage zone.

Fig. 3.3 is a plot of the length of the damage zone versus decreasing depth of focus displaying this trend. As the surface is reached, the absorption is dominated by surface absorption. As air has a much lower thermal conductivity than silicon, the surface will heat faster at a given laser fluence thus creating surface damage faster than in the bulk. This has implications for the laser wafering process in that surface damage is not desirable and suggests that the optics should be designed with maximum numerical aperture to reduce the laser intensity at the surface.

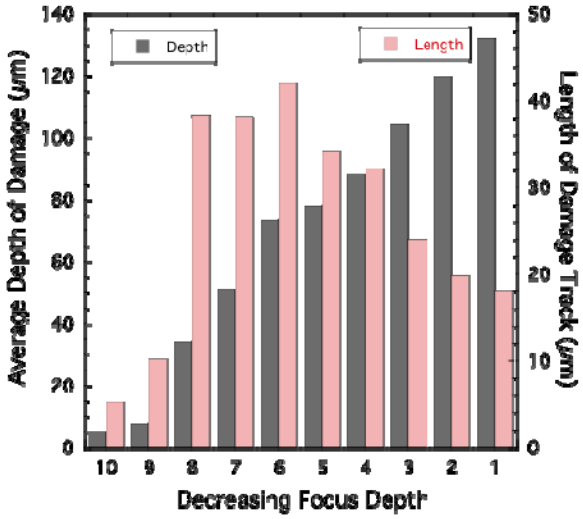

Figure 3.2 Histogram of the average damage depth and length of damage track as a function of focus depth. The focus position was adjusted to deeper depth from left to right.

To summarize, with the nanosecond laser and a conventional microscope objective, it is possible to generate subsurface laser damage in silicon. From a laser wafering perspective we note three disadvantages of this simple approach that must be overcome. First, the laser damage must be localized to a thinner region such that a planar damage zone can be generated similar to that achieved for ion implantation. Second, as the laser focus approaches the surface, there is undesirable catastrophic damage that must be avoided. Third, the breakdown events are not consistent occurring at different depths under nominally similar laser irradition conditions.

3.3. Raman Mapping

Raman spectroscopy is ideally suited for quantifying subsurface laser damage in silicon. The peak position is sensitive to the internal stress state with compressively stressed material shifted to higher wavenumber and tensilely stressed material to lower wavenumber. The peak width also is a measure of the disorder. Upon laser irradiation, regions that melt and subsequently solidify would be expected to show increased disorder. Using modern Raman confocal microscopy, it is possible to do a 2-dimensional mapping of a surface revealing complex details of the stress and disorder state in a sample. Implications for laser wafering are that it is important to tailor the stress state to produce conditions appropriate for inducing planar cracking.

Fig. 3.4 is a Raman map of a Si sample irradiated with the same 1064 nm laser used above. This cross section clearly shows the columnar laser damage tracks. The peak width within the columnar damage region is greater than in the bulk indicating that the Si is more disordered than the bulk silicon. The difference in peak width is not enough to indicate complete amorphization of this region, suggesting that the Si reorders upon freezing after the laser pulse, or does not completely amorphize when melting. Fig. 3.4 depicts the peak shift versus position revealing that the disordered regions are tensile relative to the bulk. This is consistent with rapid

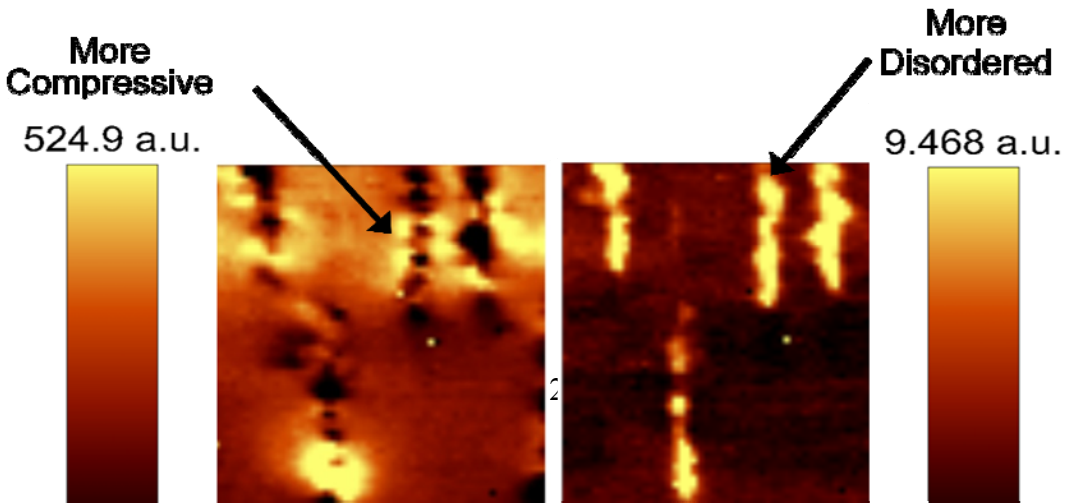

solidification leaving a slightly less dense region and thus under tension. Outside the damage track there are compressive regions. These compressively stressed regions would be ideal for providing the driving force to initiate and propagate cracks for cleaving if they could be properly controlled.

4. CONCLUSION

The purpose of this project was to lay the groundwork to develop the concept of laser wafering. Namely, that deep subsurface damage can be done by below bandgap laser radiation in silicon and that this damage can be confined to a planar region by appropriate experimental design. We have demonstrated a preliminary optic design, and shown a credible path for large array lenslet array fabrication that could be scaled to large area laser damage. These optics were fabricated and used to create subsurface damage in silicon. Preliminary laser damage studies have shown the nature of the damage tracks in silicon and the stress profiles associated with these tracks have been mapped using Raman imaging demonstrating an experimental path towards proving the efficacy of this technique.

References

[i] Applied Materials, Max Edge™ wire saw, brochure and technical specifications can be found on the web at: www.appliedmaterials.com/products/literature.html.

[ii] G. Hahn, S. Seren, M. Kaes, A. Schonecker, J.P. Kalejs, C. Dubé, A. Grenko, and C. Belouet, *Review on ribbon silicon techniques for cost reduction in PV* , Conference Record of the 2006 IEEE 4th World Conference on Photovoltaic Energy, **1** 972 (2006).

[iii] Emmanuel Van Kerschaver, Kris Baert and Jef Poortmans, *Challenges in producing photovoltaic modules on thin wafers,* Photovoltaics International, **4** 64 (2009).

[iv] A. P. Joglekar, H. Liu, G. J. Spooner, E. Meyhofer, G. Mourou, and A. J. Hunt, "*A study of the deterministic character of optical damage by femtosecond laser pulses and applications to nanomachining*," Applied Physics B **77,** 25-30 (2003).

[v] T. H. R. Crawford and H. K. Haugen, "*Sub-wavelength surface structures on silicon irradiated by femtosecond laser pulses at 1300 and 2100 nm wavelengths*," Appl. Surf. Sci. **253,** 4970-4977 (2007).

DISTRIBUTION:

5 MS1084 T.A. Friedmann, 1746
1 MS0899 Technical Library, 9536 (electronic copy)
1 MS0826 W.C. Sweat, 1535
1 MS0959 B.W. Howell, 1833